Available online at www.sciencedirect.com
ScienceDirect
Biochimica et Biophysica Acta 1773 (2007) 400–407
Biochimica et Biophysica Acta
BBA
www.elsevier.com/locate/bbamcr

Detection of MMP activity in living cells by a genetically encoded surface-displayed FRET sensor

Jie Yang [1], Zhihong Zhang [1], Juqiang Lin, Jinling Lu, Bi-feng Liu, Shaoqun Zeng, Qingming Luo *

The Key Laboratory of Biomedical Photonics of Ministry of Education, Wuhan National Laboratory for Optoelectronics, Huazhong University of Science and Technology, Wuhan 430074, PR China

Received 16 August 2006; received in revised form 30 September 2006; accepted 2 November 2006
Available online 11 November 2006

Abstract

Matrix metalloproteinases (MMPs) are secretory endopeptidases. They have been associated with invasion by cancer-cell and metastasis. Previous studies have demonstrated that proteolytic activity could be detected using fluorescence resonance energy transfer (FRET) with mutants of GFP. To monitor MMP activity, we constructed vectors that encoded a *M*MP *S*ubstrate *S*ite (MSS) between YFP and CFP. In vitro, YFP–MSS–CFP can be used to detect MMP activity and 1,10-phenathroline inhibition of MMP activity. In living cells, MMPs are secreted proteins and act outside of the cell, and therefore YFP–MSS–CFP^{display} was anchored on the cellular surface to detect extracellular MMP. A pDisplay-YC vector expressing the YFP–MSS–CFP^{display} on the cellular surface was transfected into MCF-7 cells that expressed low levels of MMP. Efficient transfer of energy from excited CFP to YFP within the YFP–MSS–CFP^{display} molecule was observed, and real-time FRET was declined when MCF-7 was incubated with MMP2. However, no such transfer of energy was detected in the YFP–MSS–CFP^{display} expressing MDA-MB 435s cells, in which high secretory MMP2 were expressed. The FRET sensor YFP–MSS–CFP^{display} can sensitively and reliably monitor MMP activation in living cells and can be used for high-throughput screening of MMP inhibitors for anti-cancer treatments.

Keywords: MMP; Fluorescence Resonance Energy Transfer (FRET); Fluorescence assay; Secretory; MMP inhibitor

1. Introduction

Proteases are necessary for the normal biological function of mammalian cells and have been associated with many pathological processes, such as wound healing, inflammation, and tumour invasion. Matrix metalloproteinases (MMPs) are a family of secretory endopeptidases with hydrolytic activity for a diverse spectrum of extracellular proteins [1,2]. Degradation of the extracellular matrix (ECM) by MMPs aids tumour invasion [2,3]. 72 kDa MMP2 (gelatinase A) and 92 kDa MMP9 (gelatinase B) are the two MMPs most closely correlated with metastatic potential. The characters of MMP2 and MMP9 are particularly important, since they cleave collagen, the main component of basement membranes [4,5]. Several MMPs are expressed at much higher levels in cancerous tissue than in normal tissue, and the extent of expression has been shown to relate to tumour stage, invasiveness, metastasis and angiogenesis [1,6,19]. Many MMP inhibitors have been designed to treat malignancies and other diseases associated with pathologic angiogenesis, including several currently in clinical development for cancer therapy, such as BB-2516, AG3340, COL-3, AE941 [1].

To study MMP activity, methods have been developed for measuring proteinase activity in vitro and in cultured cells. One of the earliest developed methods, zymography, has been used extensively; however, this method is not able to test MMP in vivo. More recently, a near-infrared fluorescence sensor that can measure enzymatic activities and provide an image of where MMP-2 is located in vivo has been designed [8,9], and this

Abbreviations: MMP, Matrix metalloproteinase; FRET, fluorescence resonance energy transfer; ECFP, enhanced cyan fluorescence protein; EYFP, enhanced yellow fluorescence protein; MSS, MMP Substrate Site; PDGFR, platelet derived growth factor receptor

* Corresponding author. Tel.: +86 27 8779 2033; fax: +86 27 8779 2034.
E-mail address: qluo@mail.hust.edu.cn (Q. Luo).
[1] These authors contributed equally to this work.

0167-4889/$ - see front matter © 2006 Elsevier B.V. All rights reserved.
doi:10.1016/j.bbamcr.2006.11.002

technique of fluorescence imaging MMP2 in vivo has had a profound impact on a variety of clinical and experimental studies. In order to test the effects of MMP inhibitors effectively in real time, MMP2, MMP9, MMP7, and MT1-MMP activities have been monitored in vitro with another fluorescence-quenched substrate, Mca–Pro–Leu–Gly–Leu–Dap(Dnp)–Ala–Arg–NH_2, at excitation and emission wavelengths of 328 and 393 nm, respectively [7]. However, the production of these probes requires complicated and costly synthetic chemical technology.

Previous studies have demonstrated that it is possible to sandwich responsive proteins between two fluorescent proteins (FPs), capable of fluorescence resonance energy transfer (FRET), and to use these proteins, as indicators, monitoring Ca^{2+} [10], cAMP [11] fluctuations and PKA activity [12], as well as protease activity [13,14] in live cells. However, it has not been reported that MMP activity has been monitored using this FP-FRET (Fluorescence Protein-FRET) method.

In this paper, we designed a genetically encoded fluorescence indicator for MMPs. It encodes a yellow fluorescence protein (YFP) and a cyan fluorescence protein (CFP) linked by a 12-amino-acid-peptide LEGGIPVSLRPV with a *M*MP *S*ubstrate *S*ite (MSS). Transfer of energy from CFP to YFP occurs because the emission spectrum of CFP overlaps significantly with the excitation spectrum of YFP. This results in YFP emission by energy transfer from CFP following CFP emission. When MMP cleave MSS site between CFP and YFP, transfer of energy from excited CFP to YFP is abolished. In living cells, a surface-anchored YFP–MSS–$CFP^{display}$ sensor can be used to detect secreted-MMP activity of the cancer cells. Consequently, this technology can be applied to screen MMP inhibitors as medicines for cancer therapy.

2. Methods

2.1. Construction of plasmids

To test MMP activity at the cell level, a mammalian expression vector pDisplay® (Invitrogen) was chosen. The pDisplay® vector was fused in two places: (1) at the N-terminus to the murine Ig κ-chain leader sequence, which directs the protein to the secretory pathway, and (2) at the C-terminus to the transmembrane domain of platelet derived growth factor receptor (PDGFR) which anchors the protein to the plasma membrane. Thus, it can display the protein under investigation on the extracellular surface. For this study, a 12-amino-acid-peptide LEGGIPVSLRPV, including the MSS site IPVS/LRPV, was chosen to link with two fluorescence proteins. The pECFP-N1 and pEYFP-N1 (Clontech Laboratories) were used as the polymerase chain reaction templates.

To express YFP–MSS–CFP in *E. coli* and cancer cells, the cDNAs of YFP and CFP coding sequence were amplified by PCR. Forward and reverse primers of EYFP were 5′-GA*AGATCT*ATGGTGAGCAAGGGCGAGGAGCTGTTCAC-3′ (restriction sites are in italics) and 5′-CG*CTCGAG*CTTGTACAGCTCGTCCATGCCGAGA-3′ respectively. Forward primers of ECFP were 5′CTCTTAGATCCGGAATGGTGAGCAAGGGCGAGGAGC3′ and 5′-CCG*CTCGAG*GGTGGAATTCCCGTGTCTCTTAGATCCGGA-3′ (the part of the linker including MMP cleavage site codons is underlined) and reverse primers and 5′-CAACTGCAG CATGCGGGCGGCGGTCACGAACTCCAGCAGG-3′ respectively. The YFP PCR products were cloned into pGEM-T (Promega), and the cloned cDNA of YFP was selected with right inserted direction; subsequently the cloned cDNA of YFP was confirmed by sequencing. Next, the CFP PCR product was digested with *Xho*I and *Pst*I, and subcloned at the *Xho*I/*Pst*I site of pGEM-T-YFP. Finally, a subclone was digested with *Bgl*II and *Pst*I, and a DNA fragment of about 1500 bp, including DNA of YFP–MSS–CFP, was cut off. This DNA fragment was inserted into the plasmid pET-28a to generate pET-28a-YC (Fig. 1A) and pDisplay to generate pDisplay-YC (Fig. 1B). Another plasmid pET-28a-YC control linker to produce YFP-SRGGGSEVNLDAE (control peptide)-CFP was also constructed to be a control.

2.2. Expression and purification of recombinant proteins

The vector pET-28a-YC and pET-28a-YC control linker were transformed into BL21 (DE3) *E. coli* (Novagen Corp.) to produce the recombinant 6His-tagged YFP–MSS–CFP and YFP-control linker-CFP. Bacteria were cultured to $A_{600}=1$ and induced with 1 mM isopropyl-1-thio-β-D-galactopyranoside (IPTG) for 16 h at 22 °C. For protein purification, cells were disrupted by sonication in 30 ml lysis buffer (20 mM Tris–Cl, pH 7.9, 0.5 M NaCl, 1 mM PMSF) followed by centrifugation (12,000×*g*, 40 min). The recombinant protein was further purified by Ni-NTA resin (Qiagen). A buffer, containing 20 mM Tris–HCl, pH 7.9, 0.5 M NaCl and 60 mM imidazole was used to remove non-specific protein. For further analysis, the recombinant FRET protein was eluted with a buffer of Tris–HCl, pH 7.9, 0.5 M NaCl and 250 mM imidazole, and dialyzed in deionized water. A 12% SDS–PAGE was used to analyze the purity of the protein. Gels were stained with Coomassie brilliant blue. Protein concentration was determined by the Folin–Phenol (Lowry) assay.

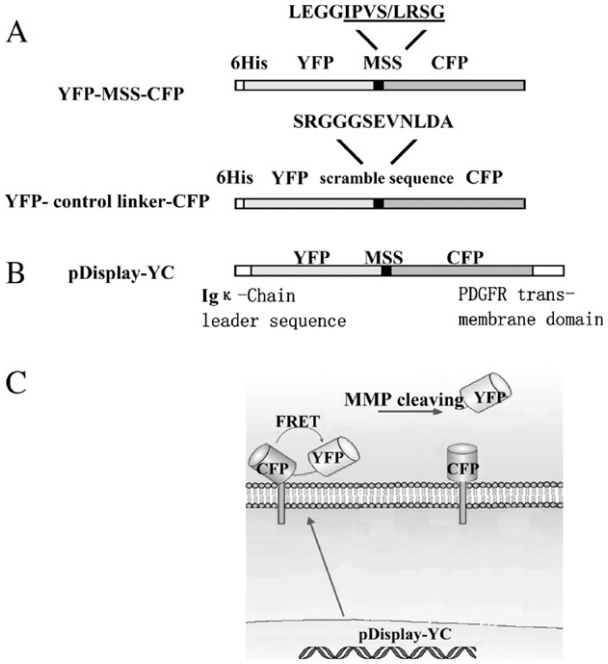

Fig. 1. Schematic representation of FP-FRET sensors for detecting MMP activity. (A) Above: the 6His-tagged YFP–MSS–CFP expressed by plasmid pET-28a-YC in *E. coli*. A twelve-amino-acid peptide LEGG*IPVSLRSG* linker includes the MMP substrate site (MSS) sequence. The MMP substrate site is IPVS/LRSG (the cleavage site is indicated by a slash [15]). Below: the 6His-tagged YFP-control linker-CFP includes scramble linker. (B) The cDNA of YFP–MSS–CFP was cloned into the pDisplay® vector, which was fused at the N-terminus to the murine Ig κ-chain leader sequence, which directs the protein to the secretory pathway, and at the C-terminus to the transmembrane domain of PDGFR, which anchors the protein in the plasma membrane, displaying it on the extracellular side. (C) Schematic representation of YFP–MSS–$CFP^{display}$ localization on the cell surface. YFP–MSS–$CFP^{display}$ is expressed and anchored on the cell membrane, where the FRET signal can be tested and active MMP can cleave the MSS sequence in YFP–MSS–$CFP^{display}$. After cleavage, the FRET and fluorescent signal of YFP will disappear.

2.3. Cell culture and gene transfection

A sample of a human breast tumour cell line MDA-MB 435s was purchased from the type culture collection of Wuhan University (Wuhan, China). Another breast tumour cell MCF-7 was kindly provided by Professor Jianfeng Liu (Huazhong University of Science and Technology, Wuhan). MDA-MB 453s and MCF-7 cells were routinely cultured in DMEM, supplemented with 10% heat-inactivated fetal bovine serum (FBS) at 37 °C in 5% CO_2.

The plasmid pDisplay-YC was transfected into MDA-MB 435s and MCF-7 cells by So-fast® transfection reagent, according to the instructions of the manufacturer (Sunma Biotechnology Corp., Xiamen City, China). After transfection, cells were selected by exposing them to G418 (Sigma) 800 μg/ml; the stable cell lines were cloned.

2.4. Fluorescence spectroscopy

The purified recombinant protein YFP–MSS–CFP was incubated with 20 nM MMP2. The reaction mixtures (pH 7.8) were transferred to a 1-cm cuvette of a spectrofluorometer (LS-50B, Perkin-Elmer, Norwalk, CT) at 37 °C. Fluorescence emission spectra from 460 to 600 nm were recorded after excitation at 433 nm (5 nm bandwidth). The FRET efficiencies were calculated by the fluorescence emission ratio of YFP (528 nm) to CFP (476 nm).

The YFP–MSS–$CFP^{display}$ expressing cells were collected and re-suspended in PBS. The cell suspensions were then done directly for fluorescence spectroscopy measurements using a spectrofluorometer. The samples were measured in a quartz cuvette. The emission spectra of the samples were collected from 460 to 600 nm (7.5 nm bandwidth), after being excited at 433 nm (5 nm bandwidth). The same amount of non-transfected cells was used as a background control.

2.5. Gelatin zymography

To assess the MMP activity in MCF-7 and MDA-MB-435s cells, gelatin zymography was performed. For the preparation of a conditioned medium for gelatin zymography, cells (at about 80% confluence) were washed three times with PBS. Cells were then cultured for an additional 24 h in a serum-free medium before collecting the conditioned medium for MMP assays. Serum-free, 24-h conditioned media as described above were collected. The collected media were centrifuged at 12,000×*g* for 3 min to remove cellular debris; 30 μl of supernatant medium was mixed with 30 μl of 2× SDS sample buffer without boiling. 30 μl of mixed samples were then electrophoresed at 4 °C on 10% SDS-polyacrylamide gel containing 0.1% gelatin. After electrophoresis, the gel was washed twice for 15 min in 2.5% Triton X-100 at room temperature to remove SDS. Finally, the gel was incubated for 16 h at 37 °C in 50 mM Tris–HCl buffer, pH 7.5, containing 200 mM NaCl and 10 mM $CaCl_2$. The gel was fixed and stained with 0.5% Coomassie blue R250 in a mixture of 30% methanol and 10% acetic acid for 15 min at room temperature, and destained with the same solution without Coomassie blue. A proteolytic band appeared clear on a blue-stained background.

2.6. Fluorescent imaging

We used an Olympus FV1000 confocal microscope (Olympus corp., JP) operating with an argon laser. The laser was tuned to lines at 458 and 515 nm. CFP was excited at 458 nm and YFP at 515 nm, Cells were examined with a 60×1.3 NA oil immersion objective and 2× zoom. The value of the ratio of FRET was calculated by using the equation R_{FRET}=FRET/CFP. The DM 505 beamsplitter directs the CFP emission to photomultiplier 1 (PMT1) and the YFP emission to photomultiplier 2 (PMT2). Emissions to each PMT were passed through a filter, specifically a bandpass for CFP emissions (BP470–500–PMT1) and a bandpass for YFP emissions (BP530–600–PMT2). The digital fluorescence images were processed using Matlab7.0 software to calculate the ratio of FRET/CFP.

Fluorescence microscopy IX-70, with a cooled CCD (Princeton) controlled by computer software Winview32 also was used to detect inhibitor effects of GM6001 and MMP2 inhibitor I (Calbiochem, Germany) on living cells. The cells were observed using a set of filters for each channel: the CFP Channel (EX. 425–445HQ, DM. 450 nm, EM.460–510HQ, Olympus corp.), the YFP channel (EX.490–500HQ, DM.505 nm, EM. 515–560HQ, Olympus corp.), and the FRET channel (EX.D436/20x, DM. 455DCLP, EM.D535/30m, Chroma corp.).

2.7. Analyzing the MMP inhibitor effect

To study the effects of the MMP inhibitor on MMP2 activity, MDA-MB 435s stably expressed pDisplay-YC were seeded into a 12-well plate with the same cell number. Cells were then treated with 40 μM GM6001 or 10 μM MMP2 inhibitor MMP2 inhibitor I (Calbiochem, Germany); control cells were added into PBS. The fluorescence signal of each group of cells was recorded through the filter cube of CFP, YFP and FRET in an Olympus IX70 inverted microscope.

2.8. Western blotting

Cells were collected at 800 rpm for 8 min and washed with phosphate-buffered saline (PBS). The cell pellets were re-suspended in lysis buffer (62.5 mM Tris–HCl, pH 6.8, 10% (v/v) glycerin, 2% (w/v) SDS, 1 mM phenylmethylsulfonyl fluoride). The extract of cell were immediately incubated for 10 min at 95 °C. Proteins were separated in the 10% SDS-PAGE, and subsequently transferred onto a polyvinylidene difluoride membrane (PVDF, Amersham) with a semi-dry blotting system. Following blotting, the membrane was probed with an anti-GFP antibody (1:2000) (Clontech) in TBST with 0.5% Tween-20. The immunoblot was then probed with goat anti-rabbit IgG-horseradish peroxidase-conjugate (1:5000) (Bio-Rad), and the bands were detected using the ECL Western blotting analysis system (Amersham).

3. Results

3.1. Characterization of the recombinant FRET sensor in vitro

The cDNA of YFP–MSS–CFP and CFP-control linker-YFP were inserted into pET-28a (Fig. 1A), which is able to express the recombinant YFP–MSS–CFP and CFP-control linker-YFP in *E. coli* BL21 (DE3) when induced with IPTG. 6His-tagged YFP–MSS–CFP, CFP-control linker-YFP and MMP2 were purified through a Ni-NTA column after induction with 1 mM IPTG.

To prove the ability of the FRET sensor YFP–MSS–CFP to detect the activity of MMP2, 6His-tagged YFP–MSS–CFP and MMP2 were mixed; the kinetic effect of MMP2 on YFP–MSS–CFP was detected using the spectrofluorometer at 37 °C. Fig. 2A shows the emission spectra of purified YFP–MSS–CFP, recorded with an excitation wavelength of 433 nm. The two emission peaks of YFP–MSS–CFP occurred at 476 nm and 528 nm, and fluorescence intensity ratio of 528/476 nm was 4.5. This result indicates that strong FRET from CFP to YFP occurred. After adding 20 nM MMP2 to the solution of YFP–MSS–CFP, a significant decrease of emission at the wavelength of 528 nm was observed during each 2-min scanning interval. The ratio of 528 to 476 gradually decreased as time elapsed. Then we also kinetically monitored production of cleaved products by SDS-PAGE (as showed in Fig. 2B). The result showed that YFP–MSS–CFP was gradually cleaved by MMP2. Meantime, two approximate 31 kDa bands (CFP and YFP) were accumulated and became dominant after proteolytic reaction.

In order to confirm further the ability of the purified sensor to measure MMP activity, a broad–spectrum MMP inhibitor, 1,10-phenathroline, a zinc chelator [22], was used to inhibit the effects of MMP2 on YFP–MSS–CFP. Fig. 2C shows the

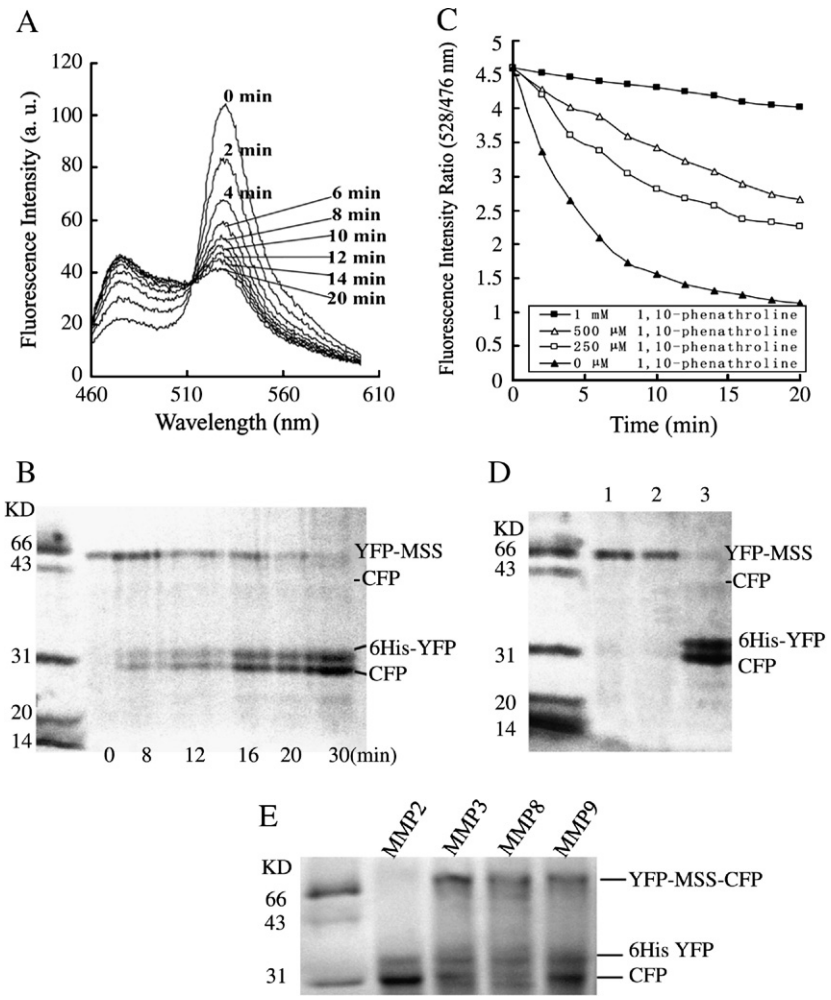

Fig. 2. Characterization of the recombinant FRET sensor in vitro. (A) 6His-tagged YFP–MSS–CFP was incubated with MMP2 (concentrations 20 nM) at 37 °C. Fluorescence emission spectra were recorded after excitation at 433 nm. (B) 6His-tagged YFP–MSS–CFP in a buffer (10 mM pH 8.0 Tris–HCl, 5 mM $CaCl_2$ and 1 μM $ZnCl_2$) and 20 nM MMP2 was added and digestion took place at 37 °C. At times indicated in the figure, aliquots of the reaction mixture were removed, quenched by boiled in water, and analyzed by 12% PAGE gel. (C) Purified YFP–MSS–CFP was used to detect inhibition by different concentrations of 1,10-phenathroline (0 μM, 250 μM, 500 μM and 1 mM). 20 nM MMP2 was incubated with 3.5 μM YFP–MSS–CFP and different concentrations of 1,10-phenathroline. The relative fluorescence ratio (528/476 nm) was plotted at each time. (D) SDS-PAGE electrophoresis demonstrates the cleavage of YFP–MSS–CFP. The samples were purified 6His-tagged YFP–MSS–CFP after incubation for 40 min with mature MMP2 in the presence (+) (lane 1) and absence (−) (lane 3) of 1 mM 1,10-phenathroline at 37 °C. The products of YFP-scramble linker-CFP incubated with MMP2 are shown in lane 2. (E) MMP2, MMP3, MMP8, MMP9 with equal activity unit were individually incubated with 10 μM YFP–MSS–CFP for 1 h. Then the products were run in 12% SDS-PAGE gel after boiled.

change over time of the relative fluorescence ratio of YFP to CFP in the solution of YFP–MSS–CFP and 20 nM MMP2 pre-incubated with 250 μM, 500 μM, and 1 mM 1,10-phenathroline, respectively. When 1,10-phenathroline was absent, the emission ratio of 528/476 nm dramatically decreased. However, the emission ratio of 528/476 nm decreased only slightly when we used a high concentration of 1,10-phenathroline (1 mM) to inhibit the MMP2 activity. These results confirm that the FRET sensor YFP–MSS–CFP is a valid measuring device, sensitive enough to monitor MMP2 activity in vitro, and able to rapidly and conveniently evaluate and screen MMP inhibitors.

Subsequently, we also analyzed it using SDS-PAGE. Fig. 2D shows that YFP–MSS–CFP remained intact when YFP–MSS–CFP was incubated with MMP2 in the presence of 1 mM 1,10-phenathroline (lane 1). The YFP-control peptide-CFP was not either cleaved by MMP2 (lane 2). However, when YFP–MSS–CFP was incubated with MMP2 in the absence of 1,10-phenathroline (lane 3), it was cleaved. This result verifies that MMP2 cleaved YFP–MSS–CFP into YFP and CFP, and that 1,10-phenathroline could inhibit MMP2 activity.

Next, we examined the sensitivity of YFP–MSS–CFP for MMPs in vitro. MMPs have been reported to exhibit some overlap in substrate specificity [15]. IPVS-LRSG peptide is cleaved at greatest rate by MMP-2 [15]. We incubated the YFP–MSS–CFP against a panel of MMP: MMP-2, MMP-3, MMP-8, and MMP-9. Fig. 2D showed MMP3, MMP8, and MMP9 have a part of activity for YFP–MSS–CFP when compared with MMP2. Human β-secretase (β-site APP-cleaving enzyme, Sigma) was added to the control experiment with no cleavage products observed (data not shown).

3.2. Surface-displayed fluorescence sensor in cancer cells

MMP are secreted as the proenzyme and can completely degrade the extracellular matrix components once activated [16]. To test MMP at the cell level, we chose a vector pDisplay®, a mammalian expression vector. In the experiments, the pDisplay carried a murine Ig κ-chain leader sequence at the N-terminus, directing the protein to the secretory pathway, and a transmembrane domain of PDGFR at the C-terminus, which anchors the protein to the plasma membrane. Consequently, cDNA of YFP–MSS–CFP sequences were inserted into pDisplay to produce pDisplay-YC (Fig. 1B). pDisplay-YC expresses YFP–MSS–$CFP^{display}$ in the cancer cells that can be anchored on the cellular surface, where fluorescence sensors can be cleaved by secreted MMP (Fig. 1C). After cleavage, YFP was cut off and moved away from the cellular surface, while CFP remained anchored on the surface of the plasma membrane. Therefore, decreased FRET efficiency or YFP fluorescent signal in YFP–MSS–$CFP^{display}$ expressing cells could reflect the activity of MMP.

MCF-7 cells were transfected with pDisplay-CFP, pDisplay-YFP and pDisplay-YC (Fig. 3). The confocal sections of imaging show that the fluorescence proteins surround the cell. Emission from CFP was detected as strong fluorescence in the CFP channel (470–500 nm, excited at 458 nm), no bleed-through fluorescence in the YFP channel (530–600 nm, excited at 515 nm) and a little bleed-through in FRET channel (530–600 nm, excited at 458 nm). Meanwhile, YFP was detected as strong fluorescence in the YFP channel and no bleed-through into the CFP channel and only a little into the FRET channel. YFP–MSS–$CFP^{display}$ was detected as strong fluorescence in all channels.

3.3. Testing different cell lines for MMP expression

MMP are constitutive expression proteins in many different cancer cell lines. For this study, we chose two kinds of cell lines, MDA-MB 435s and MCF-7 cells. Zymography was employed to analyze metalloproteinases in conditioned supernatants of MDA-MB 435s and MCF-7 cells. Fig. 4A shows that the MDA-MB 435s breast cancer cell line produced MMP with 72 kDa and 92 kDa; these results are consistent with the characteristics of latent MMP2 and MMP9. However, these two molecules couldn't be detected in MCF-7 cell line. Consequently, we used MCF-7 cells as a control to analyze MMP activity.

Fig. 4B displays the emission spectra of YFP–MSS–$CFP^{display}$ expressing MDA-MB 435s and MCF-7 cells excited at 433 nm. YFP–MSS–$CFP^{display}$ expressing MCF-7 cells peaks at 528 nm, but YFP–MSS–$CFP^{display}$ expressing MDA-MB 435s cells does not peak at this wavelength. Single cell fluorescence images of MDA-MB-435s and MCF-7 cells were acquired through a three-filter method. YFP–MSS–$CFP^{display}$ expressing MDA-MB 435s cells showed much lower fluorescence intensity in the YFP channel than YFP–MSS–$CFP^{display}$ expressing MCF-7 cells (data not shown). The reason for this phenomenon is that the MDA-MB-435s cells secrete MMP into the conditioned medium. Consequently, YFP is cut off and diffuses into the conditioned medium, resulting in the FRET's disappearance.

3.4. Real-time FRET detecting MMP2 activity

In the next set of experiments, we investigated the FRET ratio of FRET sensor YFP–MSS–$CFP^{display}$ at the single cell level. MCF-7 cells transfected with pDisplay-YC were exposed to 0.2 μM MMP2 in a conditioned medium, and CFP and FRET

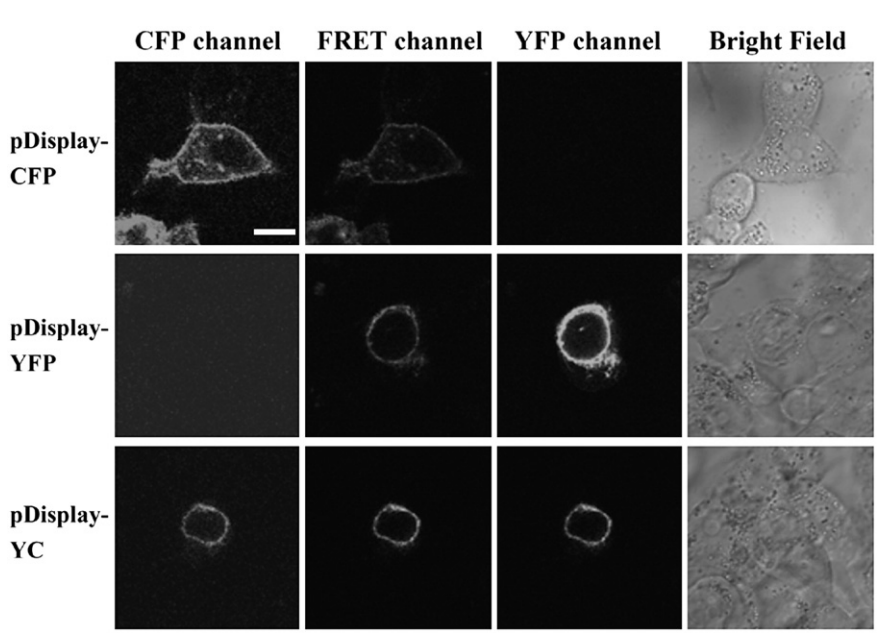

Fig. 3. Confocal imaging of MCF-7 transfected with pDisplay-CFP (top row), pDisplay-YFP (bottom row) and pDisplay-YC (bottom row). The fluorescent signals were recorded in CFP channel (470–500 nm, excited at 458 nm), FRET channel (530–600 nm, excited at 458 nm), and YFP channel (530–600 nm, excited at 515 nm), respectively. Confocal imaging shows that the fluorescence proteins surround the cell. Scale bar = 10 μm.

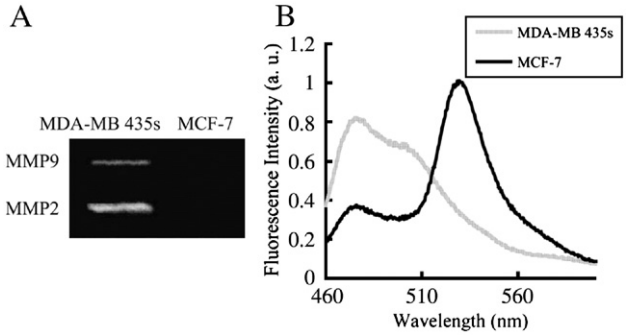

Fig. 4. Detecting MMP activity in MDA-MB 435s and MCF-7 cells. (A) To detect the MMP activity in the cancer cells by gelatin zymography, the equal amounts of conditioned medium of MDA-MB 435s and MCF-7 cells were analyzed. Cells were washed three times with PBS. Cells were then cultured for 24 h in a serum-free medium before collecting the conditioned medium for MMP assays. The collected media were centrifuged at 12,000×*g* for 3 min to remove cellular debris and 30 μl of the supernatant was mixed with 30 μl of 2× SDS sample buffer without boiling. 30 μl of mixed samples were then electrophoresed at 4 °C on 10% SDS-polyacrylamide gel containing 0.1% gelatin. After electrophoresis, the gels were washed twice for 15 min in 2.5% Triton X-100 at room temperature to remove SDS. Finally, the gel was incubated for 16 h at 37 °C in 50 mM Tris–HCl buffer, pH 7.5, containing 200 mM NaCl and 10 mM $CaCl_2$. The gel was fixed and stained with Coomassie blue R250, and destained with the same solution without Coomassie blue. A proteolytic band appeared clear on a blue-stained background. (B) YFP–MSS–$CFP^{display}$ expressing MDA-MB 435s and MCF-7 cells were excited at 433 nm and emission spectra were recorded and normalized.

fluorescence signals were recorded by confocal microscopy (Fig. 5A). In Fig. 5B, pseudo-color images demonstrate that the emission ratio, FRET/CFP, decreased at the MCF-7 cell surface after treated with MMP2. To validate the results of the real-time FRET ratio, Fig. 5C shows that YFP–MSS–$CFP^{display}$ was digested by MMP2 to produce a small CFP molecule (lane 2), but the sensor remained intact in the absence of MMP2 (lane 1).

3.5. Using YFP fluorescence to analyze MMP inhibitors effect

To study the effect of MMP inhibitors on MMP activity, the MDA-MB 435s cell line was chosen because it expresses high MMP level (Fig. 4A). GM6001 is a potent general MMP inhibitor [20], and MMP2 inhibitor I is a MMP2-specific inhibitor [21,23]. YFP–MSS–$CFP^{display}$ expressing MDA-MB-435s cells were treated with 40 μM GM6001 or 10 μM MMP2 inhibitor I, respectively. Control cells were not treated using MMP inhibitors. Fig. 6 shows that MMP2 inhibitor I (F3 in Fig. 6A) and GM6001 (I3 in Fig. 6A) significantly increased YFP fluorescence intensity following 72 h of treatment (Fig. 6C), in contrast to the controls (C3 in Fig. 6). The reason for this is that secreted MMP cuts off surface-displayed YFP, and YFP diffuses into the conditioned medium.

4. Discussion

In this study, we constructed a genetically encoded surface-displayed FRET sensor that was successfully used to monitor MMP cleavage activity and to analyze MMP inhibitor effects both in vitro and in living cells. Although zymography can be employed to analyze MMP2 and MMP9 activity, in this study, genetically encoded surface-displayed FRET sensor combined with FRET imaging technique showed more flexibility and reliability in monitoring MMP activity in vitro and in living cells. It should be noted that these recombinant FP-FRET sensor were anchored on the extracellular surface of the plasma membrane, as in a previous study where a FRET sensor was used to detect extracellular glutamate concentration [17]. Moreover, it found that the detection of YFP fluorescence intensity alone could indicate MMP activity too.

The use of FP-FRET to visualize cellular MMP expression levels has many advantages over the use of other widely used fluorescent dyes. Firstly, the FP-FRET sensor can specifically target cell organelles and cellular microenvironments [18]. Secondly, the genetically encoded FP-FRET sensors are more easily obtained and cheaper than the synthetic dyes. Thirdly, the FP-FRET method is more practical for screening novel anti-

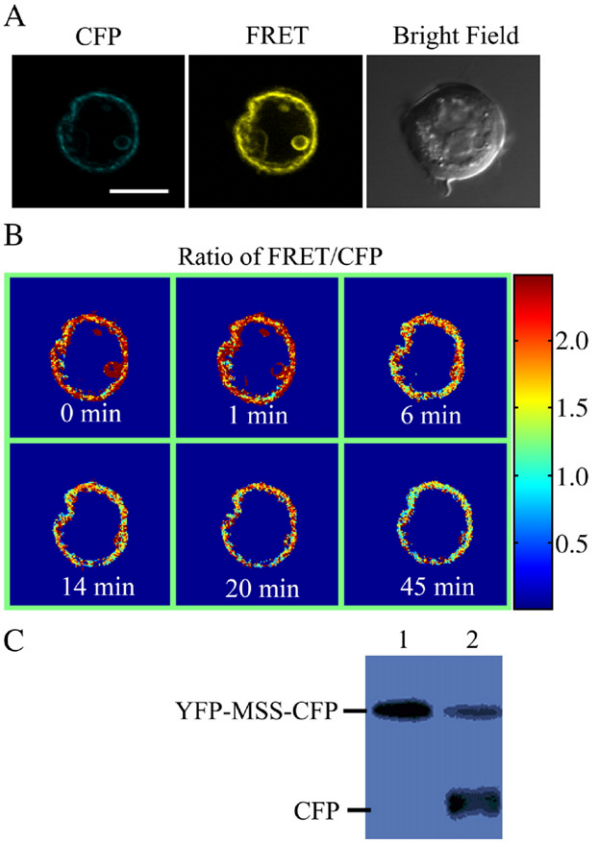

Fig. 5. Time-course FRET analysis of MMP2 activity. (A) Confocal imaging of YFP–MSS–$CFP^{display}$ expressing MCF-7 cells are shown in CFP (470–500 nm) and FRET (530–600 nm) channels and bright field. (Scale bar = 10 μm) (B) Pseudocolor imaging of FRET/CFP emission ratio at different time after the 0.2 μM recombinant MMP2 added into YFP–MSS–$CFP^{display}$ expressing MCF-7 cells. Real-time fluorescent images were monitored and the images of the FRET/CFP ratio were calculated with MATLAB 7.0. The color bar in the right panel represents the value of the ratios. (C) Western blotting shows the cleavage of YFP–MSS–$CFP^{display}$ by MMP2 in MCF-7 cells. The extract of cells was subjected to 10% SDS-PAGE and western blotting with an anti-GFP antibody. The upper blot indicates YFP–MSS–$CFP^{display}$ and the lower blot indicates CFP. Lane 1, control (MMP2 absent); Lane 2, the cells were incubated with MMP2. (For interpretation of the references to colour in this figure legend, the reader is referred to the web version of this article.)

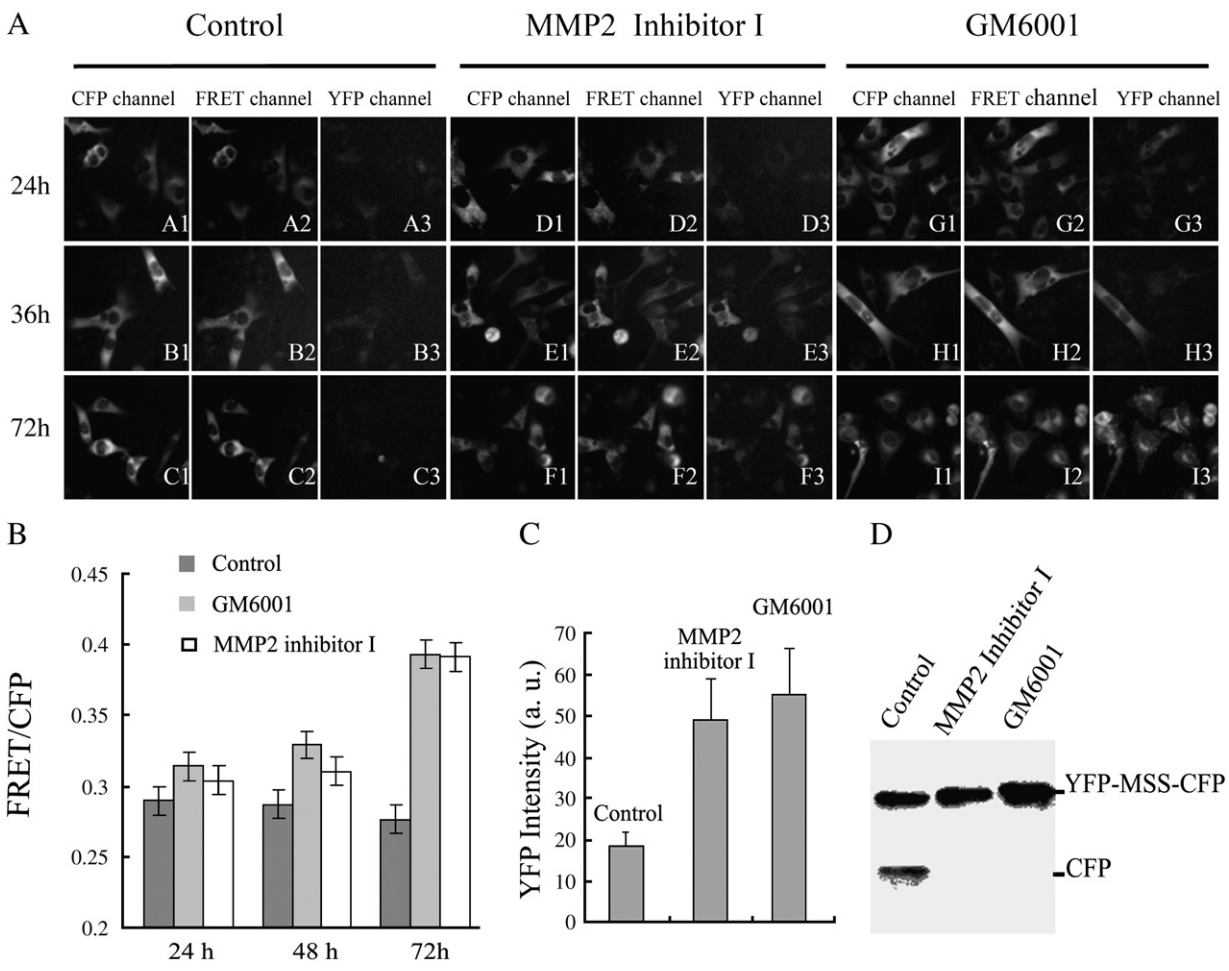

Fig. 6. Using YFP fluorescence to analyze the effects of MMP inhibitors. (A)YFP–MSS–CFP^{display} stably expressing MDA-MB 435s were treated with 10 μM MMP2 inhibitor I (D–F) and 40 μM GM6001 (G–I) and control (A–C). Cell fluorescence was detected every 24 h (24 h, top row; 48 h, middle row; 72 h, bottom row) with the 3-channel method. CFP, YFP, and FRET signals were recorded. MMP2 inhibitor I (E3, F3) and GM6001 (H3, I3) significantly increased YFP fluorescence intensity following 24–72 h of treatment, in contrast to the controls (B3, C3). (B) Ratio analysis of FRET/CFP when using MMP2 inhibitor I and GM6001 and no inhibitor (Control) to treat MDA-MB 435s cells. Data are mean±SEM for one representative experiment in twelve cells. (C) Analysis of YFP intensity after 72 h of inhibitor treatment and control. Data are mean SEM for one representative experiment in twelve cells. (D) Western blotting analysis of the sensor using MMP inhibitors 72 h treatment as described in panel A.

MMP drugs. The assay can be performed in a convenient 96-well microplate format using purified enzymes and can be developed for high-throughput systems. This assay is useful to screen drug targets or inhibitors of MMP-2, a potential therapeutic target. Consequently, we designed a genetically encoded FP-FRET sensor that could be used to detect MMP activity and applied it to evaluate the effects of MMP inhibitors in living cells.

During molecular sensor detection in vitro, the emission ratio (528/476 nm) of FRET sensor showed a 4.3 fold decrease when the FRET sensor cleaved by MMP2. A large change of the FRET ratio evidenced that YFP–MSS–CFP can be used to sensitively detect MMP2 activity. Furthermore, this method can monitor effects of MMP inhibitors in real time. Accurate information on biological digestion processes can be made visible. In vitro, we chose 1,10-phenathroline to inhibit the MMP2, but it was not chosen for living cells because of its cytotoxicity.

The above results indicate that MMP enzyme activity can be recorded through the use of fluorescent protein FRET sensor. Two cell lines, MCF-7 with low level of secreted MMP, and MDA-MB 435s with high MMP expression, were stably transfected with pDisplay-YC in order to monitor the FRET signal. The FRET signal in MDA-MB 435s was dramatically weaker than in the MCF-7 cell. Real-time FRET was also analyzed with YFP–MSS–CFP^{display} expressing MCF-7 cells after adding purified MMP2 to the cells. Finally, analysis of the YFP channel in a single cell showed that the two MMP inhibitors, GM6001 and MMP2 inhibitor I, could both inhibit MMP2 activity.

In previous studies, most FRET reactions were within the cell, not at the cell surface. However, when the FRET sensor was expressed within the cell, the quantity of FRET acceptor molecules would not change when FRET sensors were cleaved because intact cell organelles sealed off all of the molecules. In contrast, when the FRET sensor was expressed on the cell surface to detect MMP, the quantity of FRET acceptor molecules would decrease since they diffuse away from the cell membrane. Therefore, besides FRET ratio analysis of MMP

activity, an acceptor signal can also be used to analyze MMP activity.

Fluorescence detection of proteinase activity has two important applications—the analysis of the biological functions of proteinases and the screening of specific inhibitor drugs. Highly sensitive and specific synthetic fluorogenic substrates have been used for high-throughput screening of small-molecule inhibitors. Future studies involving fluorescence assays of MMP inhibitors in live tissue will provide a platform for high-throughput screening of MMP inhibitors.

Acknowledgments

This work was supported by National Natural Science Foundation of China (Grant No. 60440420131), National Key Basic Research Special Foundation of China (973 Program: 2004CB520804), and the National Key Technologies Research and Development Program of China (2005BA711A04). We thank Qiushi Yi and Qian Liu for editing the FRET analysis software and Dr. Deyun Qiu (Huazhong Agriculture University of Wuhan) and Professor Qingming Wang (Capital Medical University, Beijing, China) for providing bacteria and plasmids.

References

[1] M. Egeblad, Z. Werb, New functions for the matrix metalloproteinases in cancer progression, Nat. Rev., Cancer 2 (2002) 161–174.
[2] J.S. Rao, Molecular mechanisms of glioma invasiveness: the role of proteases, Nat. Rev., Cancer 3 (2003) 489–501.
[3] A.R. Nelson, B. Fingleton, M.L. Rothenberg, L.M. Matrisian, Matrix metalloproteinases: biologic activity and clinical implications, J. Clin. Oncol. 18 (2000) 1135–1149.
[4] M.A. Moses, The regulation of neovascularization of matrix metalloproteinases and their inhibitors, Stem Cells 15 (1997) 180–189.
[5] M. Nguyen, J. Arkell, C.J. Jackson, Human endothelial gelatinases and angiogenesis, Int. J. Biochem. Cell Biol. 33 (2001) 960–970.
[6] G. Bergers, R. Brekken, G. McMahon, T.H. Vu, T. Itoh, K. Tamaki, K. Tanzawa, P. Thorpe, S. Itohara, Z. Werb, D. Hanahan, Matrix metalloproteinase-9 triggers the angiogenic switch during carcinogenesis, Nat. Cell Biol. 2 (2000) 737–744.
[7] S. M.M.Bernardo, Z.H. Brown, R. Li, S. Fridman, Synthesis and characterization of potent, slow-binding inhibitors that are selective for gelatinases, J. Biol. Chem. 271 (1996) 17119–17123.
[8] C. Bremer, C.H. Tung, R. Weissleder, In vivo molecular target assessment of matrix metalloproteinase inhibition, Nat. Med. 7 (2001) 743–748.
[9] C. Bremer, S. Bredow, U. Mahmood, R. Weissleder, C.H. Tung, Optical imaging of Matrix Metalloproteinase-2 activity in tumors: feasibility study in a mouse model, Radiology 221 (2001) 523–529.
[10] A. Miyawaki, O. Griesbeck, R. Heim, R.Y. Tsien, Dynamic and quantitative Ca^{2+} measurements using improved cameleons, Proc. Natl. Acad. Sci. U. S. A. 96 (1999) 2135–2140.
[11] M. Zaccolo, F. De Giorgi, C.Y. Cho, L. Feng, T. Knapp, P.A. Negulescu, S.S. Taylor, R.Y. Tsien, T. Pozzan, A genetically encoded indicator for cyclic AMP in living cells, Nat. Cell Biol. 2 (2000) 25–29.
[12] J. Zhang, Y. Ma, S.S. Taylor, R.Y. Tsien, Genetically encoded reporters of protein kinase A activity reveal impact of substrate tethering, Proc. Natl. Acad. Sci. U. S. A. 98 (2001) 14997–15002.
[13] J. Lin, Z. Zhang, S. Zeng, S. Zhou, B.F. Liu, Q. Liu, J. Yang, Q. Luo, TRAIL-induced apoptosis proceeding from caspase-3-dependent and-independent pathways in distinct HeLa cells, Biochem. Biophys. Res. Commun. 346 (2006) 1136–1141.
[14] J. Lin, Z. Zhang, J. Yang, S. Zeng, B.F. Liu, Q. Luo, Real-time detection of caspase-2 activation in a single living HeLa cell during cisplatin-induced apoptosis, J. Biomed. Opt. 11 (2006) 024011.
[15] B.E. Turk, L.L. Huang, E.T. Piro, L.C. Cantley, Determination of protease cleavage site motifs using mixture-based oriented peptide libraries, Nat. Biol. 19 (2001) 661–667.
[16] L.J. McCawley, L.M. Matrisian, Matrix metalloproteinases: multifunctional contributors to tumor progression, Mol. Med. Today 6 (2000) 149–156.
[17] S. Okumoto, L.L. Looger, K.D. Micheva, R.J. Reimer, S.J. Smith, W.B. Frommer, Detection of glutamate release from neurons by genetically encoded surface-displayed FRET nanosensors, Proc. Natl. Acad. Sci. U. S. A. 102 (2005) 8740–8745.
[18] R.B. Sekar, A. Periasamy, Fluorescence resonance energy transfer (FRET) microscopy imaging of live cell protein localizations, J. Cell Biol. 160 (2003) 629–633.
[19] E. Mira, R.A. Lacalle, J.M. Buesa, G.G. Buitrago, S. Jiménez-Baranda, C. Gómez-Moutón, C. Martínez-A, S. Mañes, Secreted MMP9 promotes angiogenesis more efficiently than constitutive active MMP9 bound to the tumor cell surface, J. Cell. Sci. 117 (2004) 1847–1856.
[20] B. Winding, R. NicAmhlaoibh, H. Misander, P. Høegh-Andersen, L. Andersen, C. Holst-Hansen, A.M. Heegaard, N.T. Foged, N. Brun¨ner, J.M. Delaisse, Synthetic matrix metalloproteinase inhibitors inhibit growth of established breast cancer osteolytic lesions and prolong survival in mice, Clin. Cancer Res. 8 (2002) 1932–1939.
[21] H. Emonard, V. Marcq, C. Mirand, W. Hornebeck, Inhibition of gelatinase A by oleic acid, Ann. N. Y. Acad. Sci. 878 (1999) 647–649.
[22] F. Mannello, L. Canesi, M. Faimali, V. Piazza, G. Gallo, S. Geraci, Characterization of metalloproteinase-like activities in barnacle (*Balanus amphitrite*) nauplii, Comp. Biochem. Physiol., B 135 (2003) 17–24.
[23] Y.L. Pon, N. Auersperg, A.S.T. Wong, Gonadotropins regulate N-cadherin-mediated human ovarian surface epithelial cell survival at both post-translational and transcriptional levels through a cyclic AMP/protein kinase A pathway, J. Biol. Chem. 280 (2005) 15438–15448.